Chapter 2

Pressure Drop and Boiling Heat Transfer Characteristics of R410A in Macro-Scale and Mini-Scale Channels

Jong-Taek Oh, Nguyen Ba Chien, Kwang-Il Choi and Pham Quang Vu

Additional information is available at the end of the chapter

http://dx.doi.org/10.5772/65966

Abstract

This chapter demonstrates the two-phase flow pressure drop and heat transfer of R410A during boiling in various tube types. The pressure drop and local heat transfer coefficients were obtained for heat fluxes ranging from 10 to 40 kW/m^2, mass fluxes ranging from 100 to 600 kg/m^{2}s, the vapour quality up to 1.0 and the saturation temperatures of 5–15°C. The test sections were made of various tube diameters of 1.5, 3.0, 6.61 and 7.49 mm, respectively. The effect of mass flux, heat flux, saturation temperature and inner tube diameter on pressure drop and heat transfer coefficient was analysed. The experimental results were compared against several existing pressure drop and heat transfer coefficient correlation. New correlations of pressure drop and boiling heat transfer coefficient were also developed in this present study.

Keywords: mini-channels, heat transfer, pressure drop, correlation, heat exchanger

1. Introduction

Mini-channels are progressively used in making the compact heat exchangers nowadays. The application of these heat exchanger types in refrigeration and air-conditioning fields shows various advantages such as higher efficiency, lower air side pressure drop, reducing refrigerant charge and the more compactness size compared to the conventional types. The development of numerous tube types enables the creation of even more effective compact heat exchangers.

At the low value of saturation temperature (normally from -30 to 20°C), say, those are typically applied in refrigeration and air-conditioning, Kim et al. [1] investigated the boiling heat transfer coefficient of R-410A in smooth/micro-fin tubes within the conditions: the saturation temperature ranged from -15 to 5°C, the mass fluxes of 70–211 kgm^2/s and the heat fluxes of 5–15 kW/m^2. In this study, the authors reported that the heat transfer coefficients increased with the increasing of heat flux and mass flux. In addition, the average heat transfer coefficients of micro-fin tubes were 80–150% and 10–60% higher than those of smooth tubes for the outside diameter (OD) of 9.52 and 7.0 mm, respectively. Kim et al. [2] demonstrated the boiling heat transfer of R-410A in horizontal copper tubes. The results were carried out in 9.52 mm OD tube with following conditions: the saturation temperature of 15°C, the heat flux of 11kW/m^2 and the mass flow of 30–60 kg/h. This study also reported that the average evaporation heat transfer coefficients of micro-fin tubes were higher than those of the smooth tubes for both refrigerants, R22 and R-410A. In the other research, Wellsandt et al. [3] reported the heat transfer coefficient and pressure drop of R410A and R407C during evaporation inside horizontal herringbone-micro-fin tubes. The authors found that, at moderate vapour quality regime, the effect of mass flux on the heat transfer coefficient was insignificant while a strong influence was observed when the vapour quality was over 60%. Inside smooth tube, the heat transfer coefficient, pressure drop and flow pattern of CO_2, R410A and R22 were investigated by Park et al. [4]. The results were reported for 6.1 mm inner diameter tube within the saturation temperature of -15 and -30°C, the mass flux of 100–400 kgm^2/s, the heat flux of 5–15 kW/m^2 and the vapour quality ranged from 0.1 to 0.8. In this study, the heat transfer coefficients of R-410A are affected by the change of heat flux, mass flux and quality. The nucleate and convective boiling heat transfer mechanisms were consequently activated.

For high evaporation temperature application such as industrial heat pump systems, Padovan et al. [5] presented the experimental results of boiling heat transfer of R134a and R410A in horizontal micro-fin tube at high saturation temperature. The wide range of testing conditions that were investigated include: the mass flux from 80 to 600 kgm^2/s, the heat flux from 14 to 83.5 kW/m^2, the vapour quality from 0.1 to 0.99 and covered the saturation temperature of 30 and 40°C. The dominance of convective boiling mechanism on heat transfer coefficient was observed at the saturation temperature of 30°C. Moreover, the effect of nucleate boiling mechanism was more distinct when the saturation temperature raised. On the other side, the heat transfer coefficient of R410A in micro-fin tube is higher than that in plain tube. This result agreed well with the others in previous studies.

In addition, beside the researches on single channel, various studies on heat transfer and pressure drop of R410A in multi-port tube have been published. Cavallini et al. [6] reported the frictional pressure gradient of R236ea, R134a and R410A inside multi-port mini-channels with the hydraulic diameter of 1.4 mm. The experimental results covered a wide range of reduced pressure from 0.1 to 0.5, and the mass flux ranged from 200 to 1400 kgm^2/s. The study showed that the existing frictional pressure drop correlations were unable to predict the data of R410A. Jatuporn et al. [7] investigated the heat transfer coefficient and pressure drop of R410A in horizontal aluminium multi-port mini-channel having the hydraulic diameter of 3.48 mm. The strong effects of mass flux, heat flux and saturation temperature on heat transfer coefficient were observed while only mass flux and saturation temperature affected on

http://dx.doi.org/10.5772/65966

pressure drop. Recently, Chien et al. [8] also reported the heat transfer and pressure drop of R410A in multi-port mini-channels with smaller hydraulic diameters, 1.14 and 1.16 mm. The data were conducted with the mass fluxes of 50–150 kgm^2/s, the heat fluxes of 3 and 6 kW/m^2 and the saturation temperature of 6°C. This study reported that only heat flux affected on heat transfer coefficient of R410A while only mass flux affected on pressure drop. A heat transfer coefficient correlation was also developed in this study.

However, due to the variation in tube geometry and diameter, the heat transfer characteristics and pressure drop of R410A during evaporation process should be experimentally validated to optimise the design of heat exchangers. In order to bring out an overview to the reader, this chapter investigates the experimental results with the wide range of operating conditions as well as the tube diameters, which have been evaluated in our lab in the past [9–11] and recently. The influence of mass flux, heat flux and channel diameter on the heat transfer coefficient and pressure drop was well reported. In addition, the comparison between the experimental results and several existing pressure drop and heat transfer coefficient correlations was carried out. Finally, the development of correlations of pressure drop and heat transfer coefficient correlations for heat exchanger with mini-channel design was demonstrated in this study.

2. Experimental facilities and data reduction

2.1. Experimental model

Figure 1(a) and **(b)** depicts the schematic diagram of the experimental apparatus for copper tube and stainless tube, respectively. In general, both facilities mainly consist of a refrigerant loop, the water loops and the data acquisition system. The refrigerant loop included the receiver tank, the sub-cool unit, the Coriolis mass flow meter, the condense unit and test sections. In boiling mode, the refrigerant was delivered clockwise by the gear pump. The mass flow rate could be controlled by changing the pump speed and was measured by the flow meter. The quality of flow was adjusted in pre-heater to the desired value before entering the test section. The test sections could be heated by a water loop or an electric transformer as shown in the figure. When using the water loop, the heat capacity could be varied by mastering the mass flow rate or temperature of inlet water. On the other hand, when using the transformer, the power could be set by controlling the input voltage. The refrigerant was then evaporated in the test section. The vapour at the outlet of test section was condensed by a condenser unit and accumulated into the receiver. The experimental apparatus was well insulated with rubber and foam to minimise the effect of surround environment temperature.

The detail of test sections for copper tube was depicted in **Figure 2(a)**. The test tubes were made from copper with the inner diameters of 6.61 and 7.49 mm. The effective length was 1200 mm. As shown in the figure, the test sections were divided into four separated sub-sections with a length of 300 mm. Along the test section, the T-type thermocouples were attached, each 150 mm of length, at three positions: top, middle and bottom. At the adiabatic pipes between two consecutive sub-sections, thermocouples and pressure transducers were

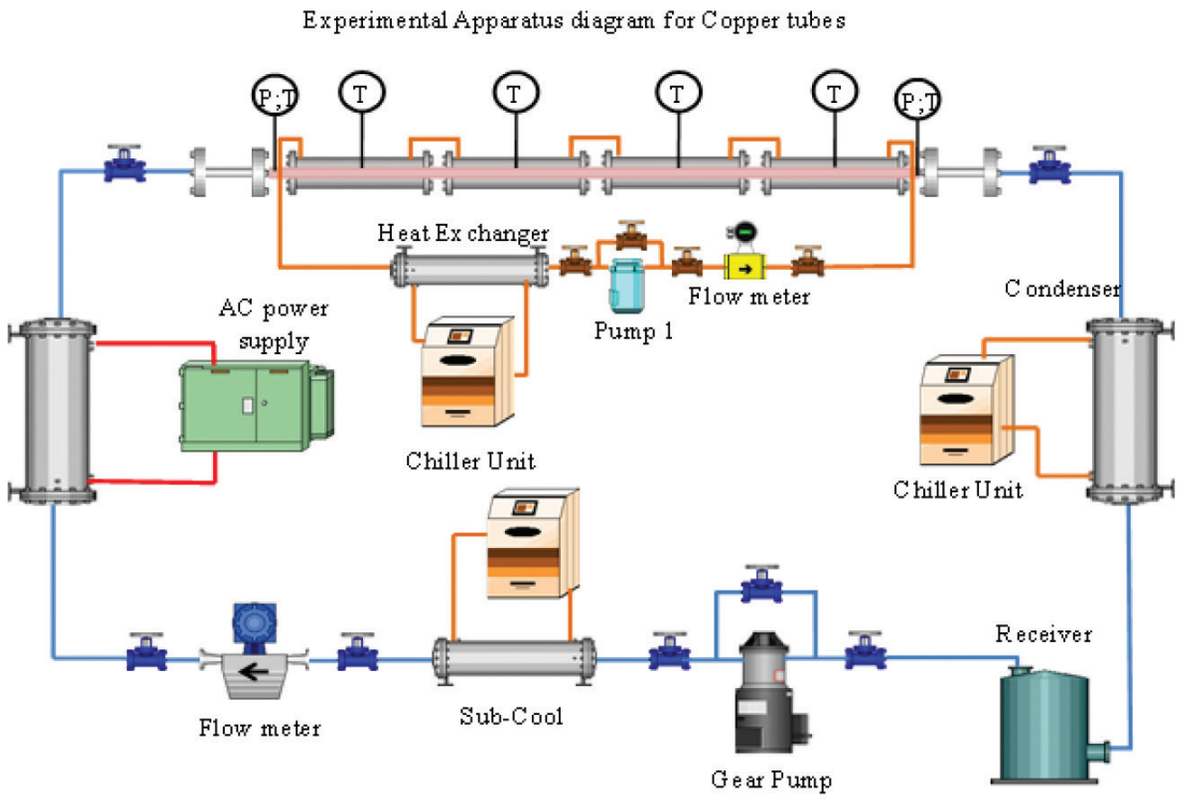

(a)

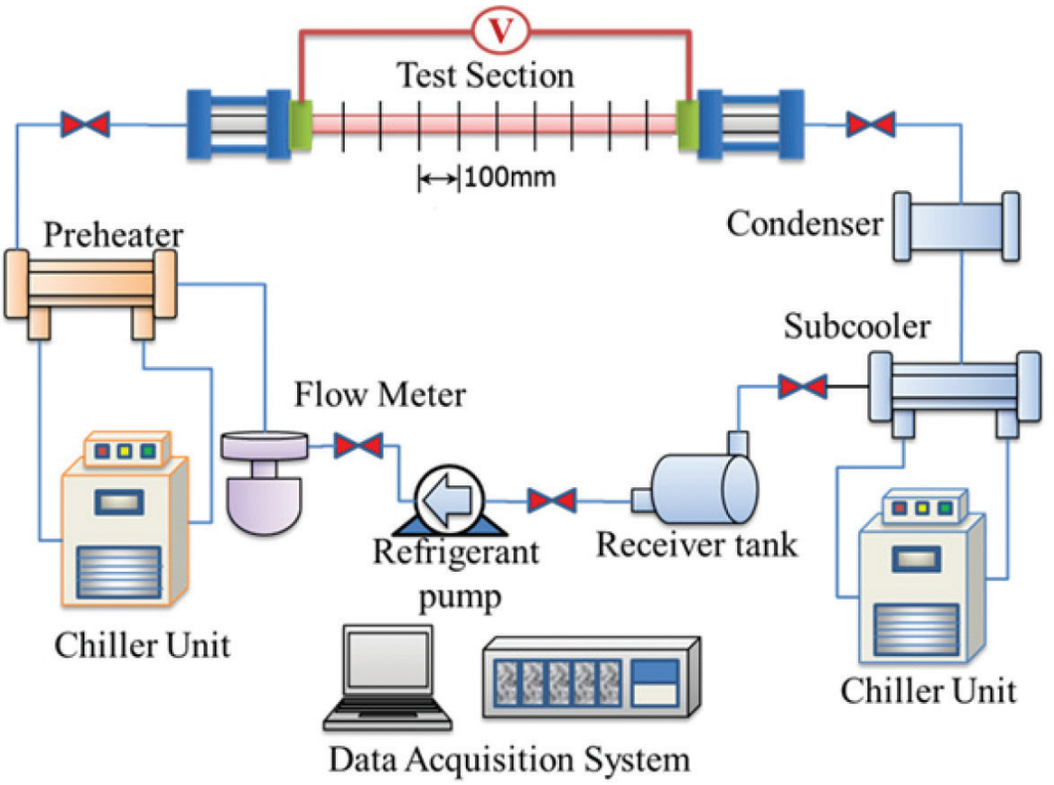

(b)

Figure 1. The experimental apparatus: (a) copper tube and (b) stainless tube.

http://dx.doi.org/10.5772/65966

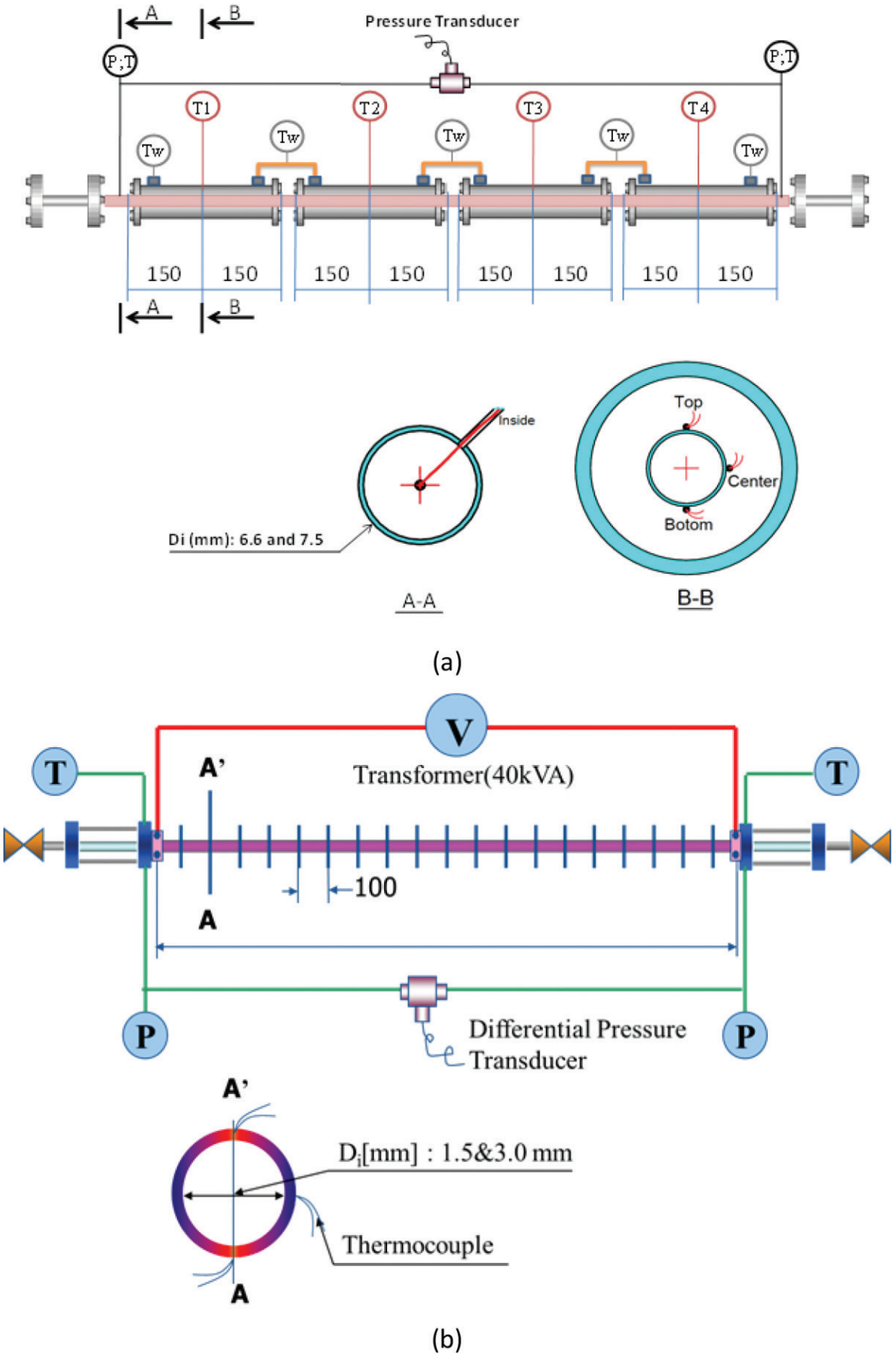

Figure 2. The test sections: (a) copper tube and (b) stainless tube.

set up to measure the local pressure drop. Two sight glasses were installed at the beginning and end of test sections to visualise the flow pattern.

Figure 2(b) describes the detail setup of test section using the stainless tube. The tubes have a diameter of 1.5 and 3.0 mm with a length of 1500 and 3000 mm, respectively. The T-type thermocouples were also attached at the top, middle and bottom points, each 100 mm, along the test section from the inlet. Two pressure transmitters were located at the inlet and outlet of the test section. To enhance the accuracy of pressure drop value, a differential pressure transducer was also set up.

The physical properties of the refrigerant were obtained from REFPROP 8 [12]. The temperature, pressure and mass flow rate data were recorded using the data acquisition.

2.2. Data reduction

The data were collected using a data acquisition and were analysed in real time by the data reduction program. All the information about test conditions and data during the operation were displayed on the monitor.

2.2.1. Heat transfer coefficient

In the case of using water heating loop, the heat capacity of each sub-section Q_n is calculated from mass flow rate and rising enthalpy of cooling water flowing inside the water tubes as follows:

$$Q_n = W_n c_p (T_{\text{nout}} - T_{\text{nin}}) - Q_{\text{loss}} \tag{1}$$

where $\dot{m}_n$, c_p, and T_n are the mass rate of flow, specific heat and temperature of cooling water in sub-section n, respectively. Q_{loss} is the heat loss on the test section, which was determined when calibrating the system. In the case of using an electric transformer, the heat capacity can be determined by the root mean square values of electric voltage and current as follows:

$$Q = I_{\text{RMS}} \times U_{\text{RMS}} \tag{2}$$

The local heat transfer coefficient inside the channel can be evaluated as the ratio of the heat flux to saturation minus the inside wall temperature:

$$h = \frac{Q}{A \times (T_{\text{wi}} - T_{\text{sat}})} \tag{3}$$

At the inlet of test section, the saturation temperatures were determined by the local measured pressures. At the outlet of each sub-section, the saturation temperatures were then calculated by subtracting the inlet temperature to the one raised by pressure drop. In the current study, the difference of temperature between the saturated refrigerant and inside wall was very high. In addition, the temperature drop raised by the pressure drop was kind of small. Therefore, the saturation temperature between the inlet and outlet of test section could be calculated as the linear function of two known values. The temperature of inside tube wall, T_{wi}, was determined based on the steady-state one-dimensional radial conduction heat transfer

http://dx.doi.org/10.5772/65966

through the wall with and without the internal heat generation for the cases, heat flux was applied by the electric transformer and hot water, respectively.

The vapour quality, x, at the measurement locations, z, was determined based on the thermodynamic properties:

$$x = \frac{i - i_f}{i_{fg}} \tag{4}$$

In some cases, since the refrigerant flow could not be saturated completely before entering the test section, the sub-cooled length was determined as follows:

$$z_{sc} = L\frac{i_f - i_{fi}}{\Delta i} = L\frac{i_f - i_{fi}}{(Q/W)} \tag{5}$$

2.2.2. Pressure drop

The total pressure drop of two-phase fluid in general is calculated by the sum of the static head Δp_{static}, the momentum $\Delta p_{\text{momentum}}$ and the frictional pressure drop $\Delta p_{\text{frictional}}$:

$$\Delta p_{\text{total}} = \Delta p_{\text{static}} + \Delta p_{\text{mom}} + \Delta p_{\text{frict}} \tag{6}$$

Since the horizontal tube was used in this study, the pressure head can be neglected. The saturated refrigerant from liquid is evaporated linearly with the test distance to vapour-liquid mixture at the vapour quality x. Therefore, the momentum pressure drop can be defined by following equation:

$$-\left(\frac{dp}{dz}a\right) = G^2\upsilon_f\left\{\left[\frac{x^2}{\alpha}\left(\frac{\upsilon_g}{\upsilon_f}\right) + \frac{(1-x)^2}{1-\alpha}\right]_{\text{out}} - \left[\frac{x^2}{\alpha}\left(\frac{\upsilon_g}{\upsilon_f}\right) + \frac{(1-x)^2}{1-\alpha}\right]_{in}\right\} \tag{7}$$

For horizontal tube, void fraction α is defined by Steiner [13] equation that was modified from Rouhani-Axelsson [14] model:

$$\alpha = \frac{x}{\rho_g}\left[(1+0.12(1-x))\left(\frac{x}{\rho_g} + \frac{1-x}{\rho_f}\right) + \frac{1.18(1-x)\left[g\sigma(\rho_f - \rho_g)\right]^{0.25}}{G\rho_f^{0.5}}\right]^{-1} \tag{8}$$

3. Result and discussions

3.1. Pressure drop

Figure 3 illustrates the significant effect of mass flux and vapour quality on pressure drop gradient of copper tube with the inner diameters of 6.61 and 7.49 mm. The pressure drops are higher with the higher mass flux. The reason can be explained in that, in horizontal tube, the

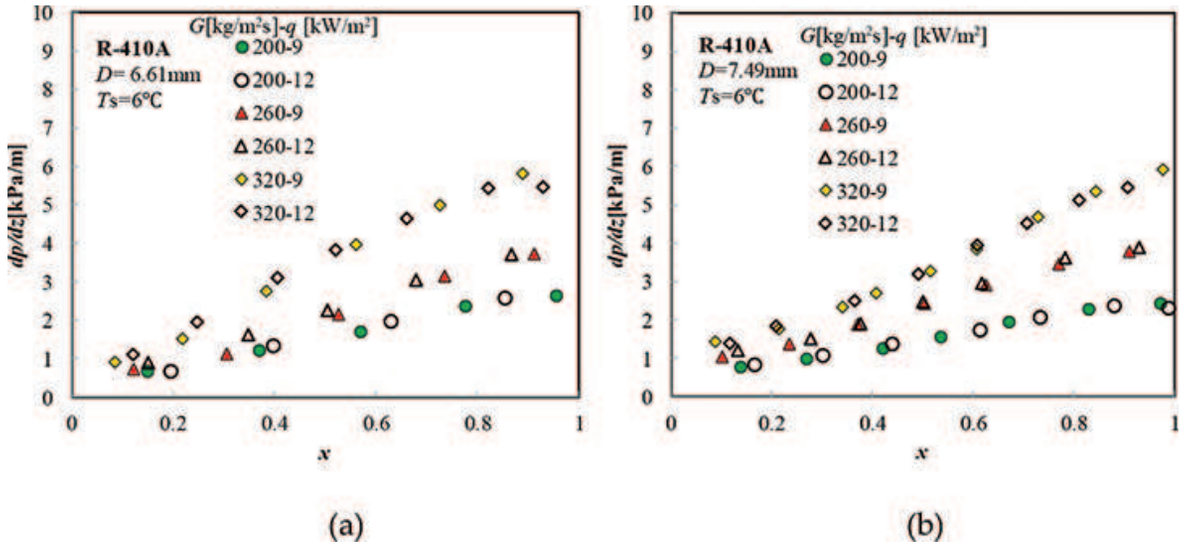

Figure 3. The effect of mass flux, heat flux and mass quality on pressure drop of R410A: (a) Di = 6.61 mm; (b) Di = 7.49 mm.

pressure drop is mainly contributed by the frictional and momentum pressure components. When the mass flux increases, the flow velocity increases, which raises both of two components. This effect of mass flux on the two-phase pressure drop was well observed in various studies including the single-mini/conventional-channel and multi-port tubes [4, 8, 15–19].

In addition, the pressure drop gradient also increases with the increase of mass quality. When the dry out occurred, the reduction in frictional pressure drop was observed. Moreover, the effect of heat flux on pressure drop is unclear.

The effects of tube diameter are depicted in **Figure 4**. The pressure drops of gradient increases when the tube diameter decreases. The wall shear stress that raises higher in smaller tube is believed to be the reason for this phenomenon.

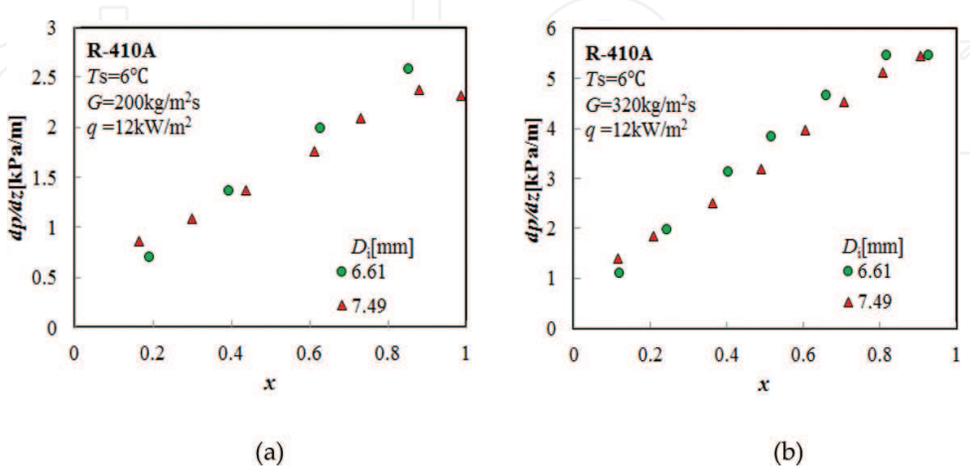

Figure 4. The effect of inner tube diameter on pressure drop of R410A: (a) G = 200 kg/m2s; (b) G = 320 kg/m2s.

http://dx.doi.org/10.5772/65966

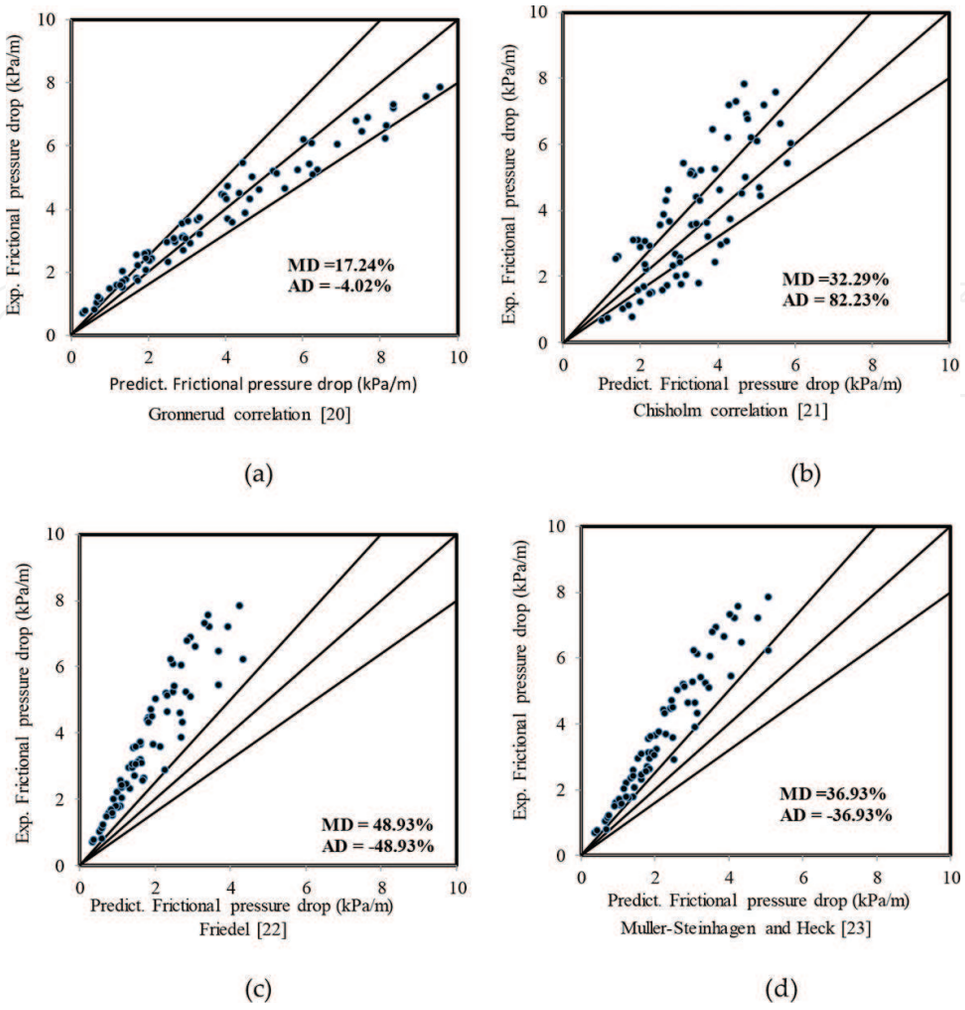

Figure 5. Comparison of experimental data with some existing frictional pressure drop correlations: (a) Gronnerud [20]; (b) Chisholm [21]; (c) Friedel [22]; (d) Muller-Steinhagen and Heck [23].

In this study, the experimental data are validated by comparing with some well-known frictional pressure drop correlations [20–23], as shown in **Figure 5**. Among them, a correlation proposed by Gronnerud [20] shows the best prediction with a mean deviation of 17.24%. His correlation determined the dependence of frictional pressure drop on the Froude number and could be applied to a wide range of mass quality from 0 to 1. Both of two correlations proposed by Chisholm [21] and Muller and Heck [23] have mean deviations of above 30%. The correlation proposed by Chisholm [21] was based on the empirical method and the one proposed by Muller and Heck [23] expressed the interpolation between the liquid and vapour flow. The correlation proposed by Friedel [22] used a wide range of data and was commended for the ratio of liquid/vapour, which is less than 1000.

In order to improve the prediction of pressure drop of R410A in horizontal tube as well as simplify the calculation, a new frictional pressure drop is developed. The general form is developed based on the ideal of Lockhart-Martinelli [24]. The frictional pressure drop is

comprised of frictional pressure drop of liquid-phase adjusted by two-phase multiplier. The equation can be determined as follows:

$$\frac{dp}{dz} f = \left(\frac{dp}{dz} F \right)_{fo} \phi_f^2 \tag{9}$$

where the frictional pressure drop of liquid phase is defined as follows:

$$\left(\frac{dp}{dz} F \right)_{fo} = \frac{2 f_{fo} G^2}{D_h \rho_f} \tag{10}$$

and f_{f_0} is frictional factor, which can be determined based on the flow regime:

$$\begin{aligned} &\mathrm{Re}_{fo} < 2300 : f_{\text{laminar}} = \frac{16}{\mathrm{Re}_{fo}} \\ &\mathrm{Re}_{fo} > 3000 : f_{\text{Blasius}} = 0.079\,\mathrm{Re}_{fo}^{-0.25} \\ &2300 < \mathrm{Re}_{fo} < 3000 : \\ &f = \frac{f_{\text{blasius}} - f_{\text{laminar}}}{3000 - 2300} (\mathrm{Re}_{fo} - 2300) + f_{\text{laminar}} \end{aligned} \tag{11}$$

From that, a regression program is developed using the experimental data as the input variable. The final factor is calculated and expressed as follows:

$$\phi_f^2 = 62.373 x^{1.086} (1 - x)^{0.151} \tag{12}$$

The proposed frictional pressure drop correlation shows a good prediction with the mean deviation of 9.29% and the average deviation of -0.69%. The comparison between the experimental data and predicting model is shown in **Figure 6**.

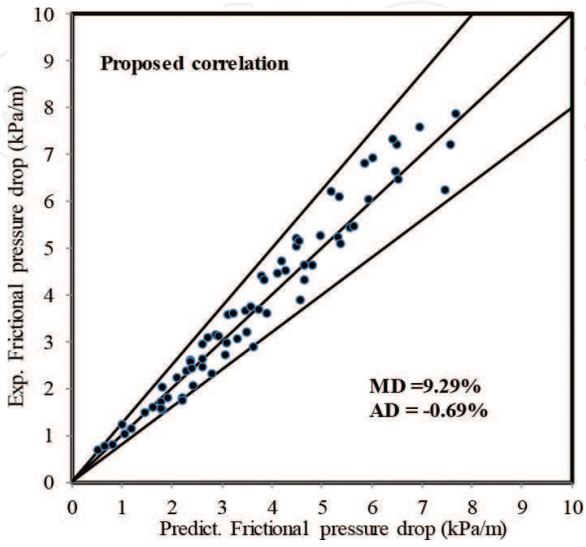

Figure 6. Comparison of experimental data with proposed frictional pressure drop correlation.

http://dx.doi.org/10.5772/65966

3.2. Heat transfer coefficient

Figure 7(a) and **(b)** illustrates the effect of mass flux on the heat transfer coefficient of R410A in 1.5 and 6.61 mm inner diameter, respectively. In low quality regime, the effect of mass flux in 1.5 mm tube, called mini-channel, is insignificant while the inverse trend of mass flux effect is shown in 6.61 mm tube, called conventional channel. It indicates that the nucleate boiling is predominant in mini-channel. The similar results are reported in other studies [10, 25–28]. The different contribution of nucleate boiling to the heat transfer coefficient of refrigerant between mini-channel and conventional channel, therefore, should be validated before applying the heat transfer model of macro-scale to mini-scale channel and vice versa. At higher quality regime, due to the active force of convective boiling, the effect of mass flux on heat transfer coefficient is clear. The higher mass flux raises the higher heat transfer coefficient.

The strong effect of heat flux on the heat transfer coefficient is shown in **Figure 8**. The trend depicts that the heat transfer coefficient of R-410A was higher with the increase in heat flux and vapour quality. The similar phenomenon was also observed in the studies of Park et al. [4] and Mastrullo et al. [29]. That means the convective boiling mechanism was active on the heat transfer mechanism of R-410A in mini-channel.

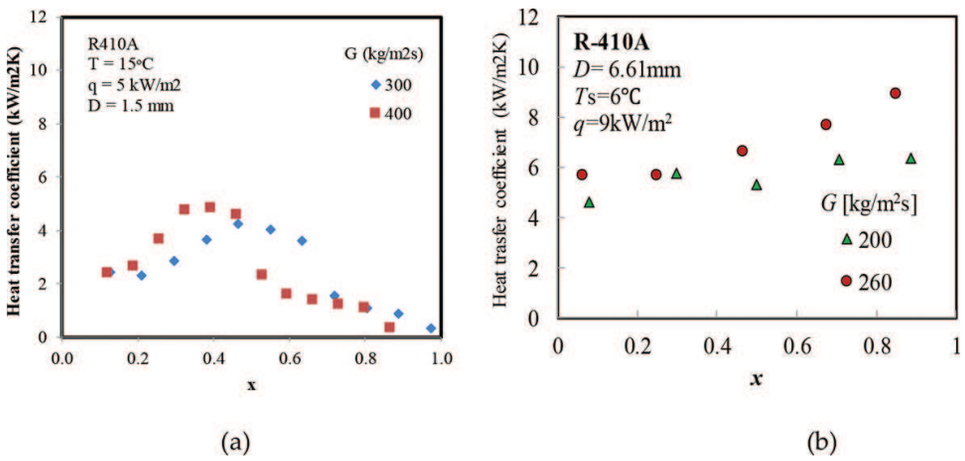

Figure 7. The effect of mass flux on heat transfer coefficient of R410A: (a) Di = 1.5 mm; (b) Di = 6.61 mm.

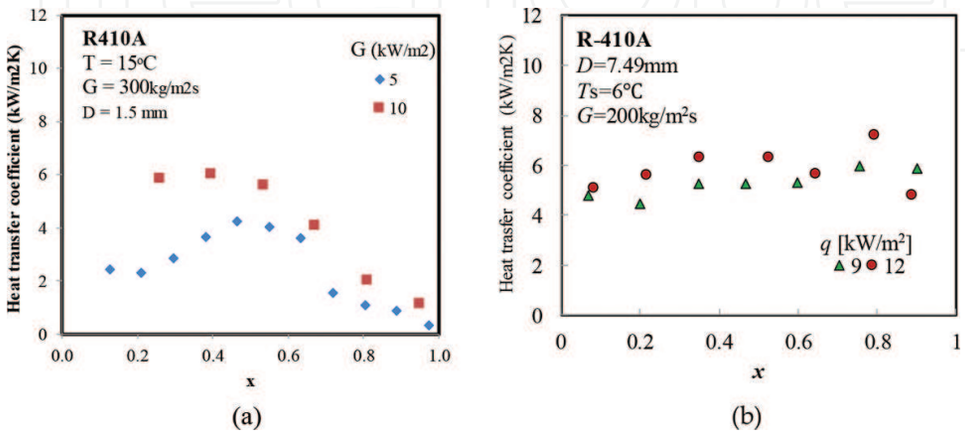

Figure 8. The effect of heat flux on heat transfer coefficient of R410A : (a) Di = 1.5 mm; (b) Di = 7.49 mm.

Figure 9 shows the effect of tube diameter on the heat transfer coefficient. The heat transfer coefficient of R410A was higher with smaller tube diameter. It can be explained that the heat transfer surface area per unit volume increases when the diameter decreases at the same operating conditions, therefore, increase the heat transfer coefficient.

In order to validate the experimental heat transfer coefficient of R410A in both mini- and macro-scale channel, Chien et al. [11] compared the data with various heat transfer coefficient correlations [26, 30–34] include both of the correlations developed for mini-scale channel and the ones developed for macro-scale channel. The data bank consists of 452 data points including 61 data with $D_h > 3.0$ mm (macro-scale) and 391 data with $D_h \leq 3.0$ mm (mini-scale). The distribution of data is depicted in **Figure 10** and the comparison is depicted in **Figure 11**. The summary of heat transfer coefficient correlation is depicted in **Table 1**. The inaccuracy of existing general heat transfer correlations in predicting the experimental data of R410A resulted due to the extrapolation of the operating condition from the previous model to the

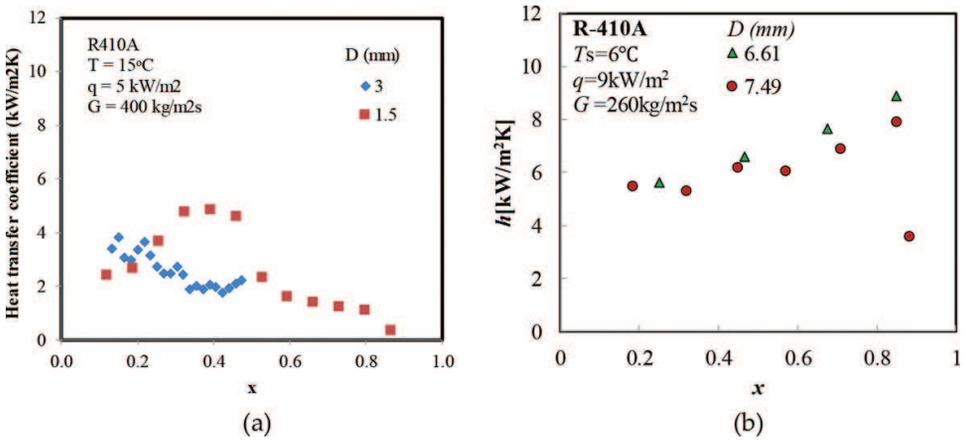

Figure 9. The effect of inner diameter on heat transfer coefficient of R410A : (a) Di = 1.5 & 3.0 mm; (b) Di = 6.61 & 7.49 mm.

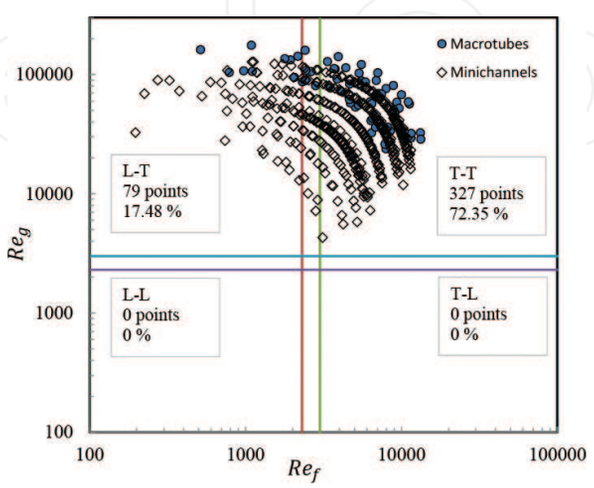

Figure 10. The data distribution.

http://dx.doi.org/10.5772/65966

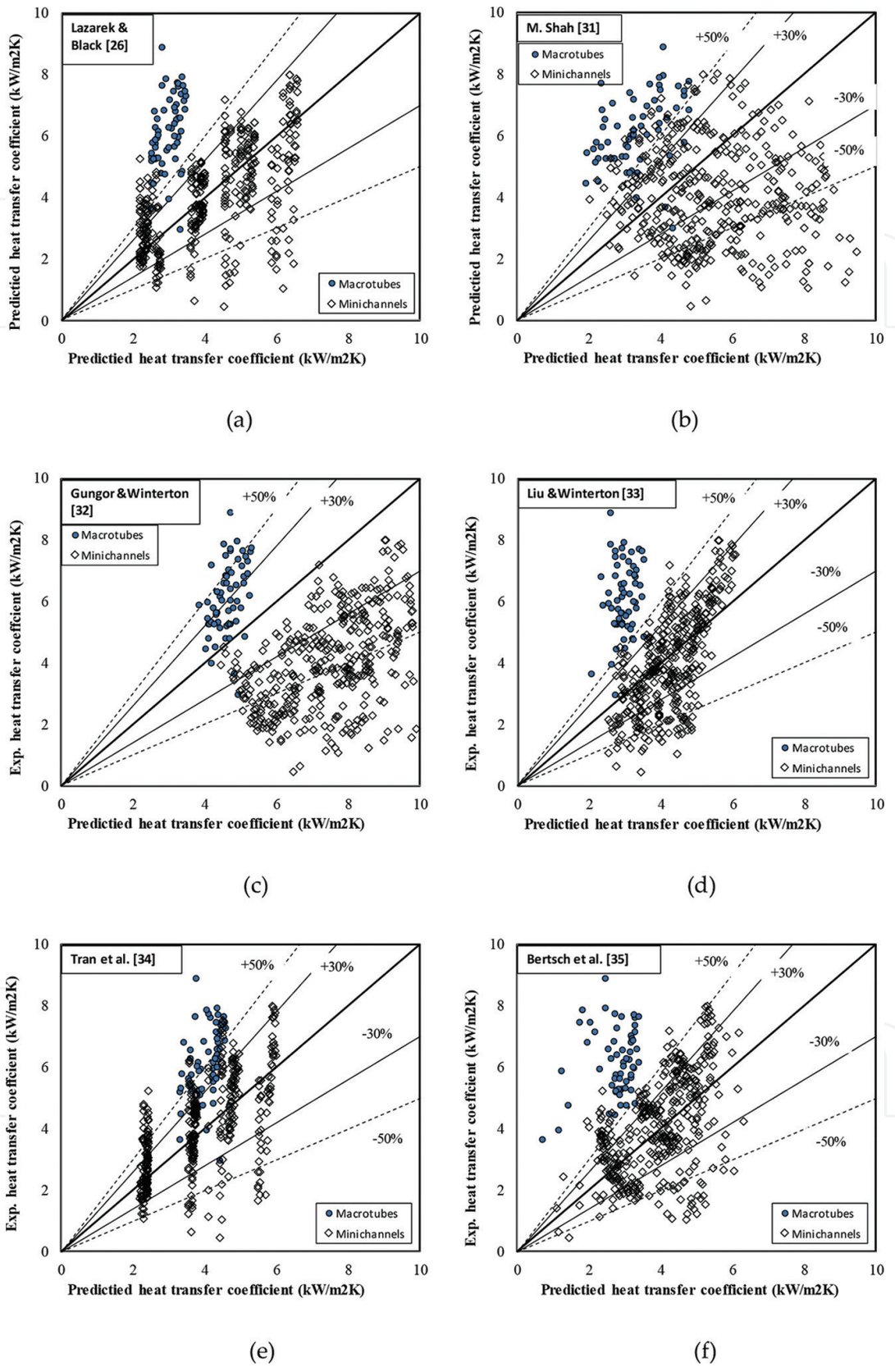

Figure 11. Comparison of experimental data with some existing correlation: (a) Lazarek and Black [26]; (b) Shah [32]; (c) Gungor and Winterton [32]; (d) Liu and Winterton [33]; (e) Tran et al. [34]; (f) Bertsch et al. [35].

1. Lazarek and Black [26] correlation	$h_{tp} = (30\mathrm{Re}_{lo}^{0.857}\, Bo^{0.714})(\frac{k_l}{D_h});$ $Re_{lo} = \frac{GD_h}{\mu_l}; Bo = \frac{\phi}{Gi_{\mathrm{lg}}}; \phi = 1.4\times10^4 - 3.8\times10^5 W/m^2$
2. Shah [30] correlation	$\psi = \frac{h_{TP}}{h_l};\ Co = \left(\frac{1}{x-1}\right)^{0.8}\left(\frac{\rho_v}{\rho_l}\right)^{0.5}$ $Bo = \frac{q}{Gh_{lv}};\ Fr_L = \frac{G^2}{\rho_l^2 gD}$ $h_l = 0.023\mathrm{Re}_l^{0.8}\,\mathrm{Pr}_l^{0.4}\left(\frac{k_l}{D_i}\right)$ $h_{tp} = \mathrm{Max}(F,S)h_l;$
3. Gungor and Winterton [31] correlation	$h_{tp} = F.h_l + S.h_{nb}$ $h_l = 0.023\mathrm{Re}_l^{0.8}\,\mathrm{Pr}_l^{0.4}\left(\frac{k_l}{D_i}\right); F = 1 + 24000Bo^{1.16} + 1.37\left(\frac{1}{X_{tt}}\right)^{0.86}$ $h_{nb} = 55P_r^{0.12}q^{2/3}(-\log_{10}p_r)^{-0.55}M^{-0.5}; S = (1+0.55F^{0.1}\,\mathrm{Re}_{lo}^{0.16})^{-1}$ If the tube is horizontal and the Froude number Fr_1 is less than 0.05 then F, S should be multiplied by the factor $F.Fr_l^{(0.1-2Fr_l)}; SFr_l^{0.5}$, respectively.
4. Liu and Winterton [32]	$h_{tp} = \left[\left(Fh_l\right)^2 + \left(Sh_{pool}\right)^2\right]^{0.5},$ $\mathrm{h}_l = 0.023\mathrm{Re}_{lo}^{0.8}\,\mathrm{Pr}_l^{0.4}\frac{k_f}{D_h}; F = \left[1 + x\,\mathrm{Pr}_l\left(\frac{\rho_l}{\rho_v} - 1\right)\right]^{0.35}$ $h_{pool} = 55P_r^{0.12}q^{2/3}(-\log_{10}p_r)^{-0.55}M^{-0.5}; S = \left(1+0.55F^{0.1}\,\mathrm{Re}_l^{0.16}\right)^{-1}$
5. Tran et al. [33]	$h = (8.4x10^{-5})(Bo^2We_l)^{0.3}\left(\frac{\rho_l}{\rho_v}\right)^{-0.4}$
6. Bertsch et al. [34]	$h_{tp} = S.h_{nb} + F.h_{conv,tp}; h_{nb} = 55P_r^{0.12}q^{2/3}(-\log_{10}p_r)^{-0.55}M^{-0.5};$ $h_{conv,tp} = h_{conv,l}.(1-x) + h_{conv,v}.x;$ $S = 1-x; F = 1 + 80.(x^2 - x^6).e^{-0.6C_f}$

Table 1. Flow boiling heat transfer correlations considered in this work.

present data as well as the significant effect of specific working fluid as proposed by Kandlikar [35, 36]. The development of a new boiling heat transfer coefficient correlation for R410A in mini- and macro-scale channels, therefore, is needed.

In general, the boiling heat transfer coefficient mainly consists of two mechanisms: the nucleate boiling and the forced convective boiling mechanism. Hence, the form proposed by Chen [37] is widely accepted and is used in this study to develop the new correlation. This form is based on the superposition model with the contribution of two heat transfer mechanisms. The formula is defined as:

$$h_{tp} = F.h_{lo} + S.h_{\mathrm{pool}} \tag{13}$$

http://dx.doi.org/10.5772/65966

In the above equation, the enhancement of convective boiling due to the increase of flow velocity when the vapour quality increases was counted by the enhanced factor F. On the other hand, the suppression of nucleate boiling term when the fluid layer thickness decrease as the vapour quality increases is defined as suppression factor S. The heat transfer coefficient of liquid phase in force convective heat transfer mechanism can be defined by the Dittus-Boelter [38] correlation as follows:

$$h_{lo} = 0.023 \mathrm{Re}_l^{0.8} \mathrm{Pr}_l^{0.4} \frac{k_l}{D} \tag{14}$$

Due to the higher velocities and the development of the thinner film layers, the heat transfer coefficients of two-phase flow are normally higher than those of single phase. For that reason, the enhancement factor F is consequently determined under the effect of the density ratio and vapour quality ratio. In the studies of Chen [37] and Gungor-Winterton [31], enhancement factor F is defined as the function of Martinelli parameter X_{tt}. Shah [30], on the other hand, replaced this parameter by convection number C_o since the influence of viscosity ratio was not found. In present study, the correlate analysis shows the same value of the Martinelli parameter and convection number on the enhancement factor. Therefore, the calculation of F can be simplified by the function of convection number $F = f(C_o)$, where the convection number was defined as follows:

$$C_o = \left(\frac{1-x}{x}\right)^{0.8} \left(\frac{\rho_g}{\rho_l}\right)^{0.5} \tag{15}$$

Using the regression method, the final form of enhancement factor F is proposed as follows:

$$F = 1.061 \exp\left(\frac{0.042}{C_o}\right) \tag{16}$$

Copper [39] developed the heat transfer correlation for nucleate boiling with the large data bank and showed a good prediction. Hence, in the remaining term, the nucleate boiling and the Copper correlation can be used to determine the pool boiling heat transfer. The equation is defined as follows:

$$h_{\mathrm{pool}} = 55 P_R^{0.12} (-\log_{10}(P_R))^{-0.55} M^{-0.5} q_H^{0.67} \tag{17}$$

Then, the suppression factor S can be modelled by a least square program. After various test, the final form of factor S is determined as the function of the convection and confinement number. The formula is expressed as follows:

$$S = 0.238 \frac{C_o^{0.238}}{C_f^{1.11}} \tag{18}$$

where the confinement number is defined as follows:

$$C_f = \frac{1}{D} \sqrt{\frac{\sigma}{g(\rho_l - \rho_g)}} \tag{19}$$

The proposed heat transfer coefficient correlation archives the mean deviation of 20.66 and 21.06% for macro-scale- and mini-scale channel, respectively. The detail comparison of the proposed correlation and the experimental data is shown in **Figure 12**. **Figure 13** summarises the overall comparison of existing heat transfer coefficient correlation and the proposed one with the present data of R410A. Among the existing correlations, the one proposed by Gungor-Winterton [31] showed the best prediction for the macro-channel with the mean deviation of 25% while this correlation failed to predict the heat transfer coefficient of mini-channel. The heat transfer coefficient correlation proposed by Tran et al. [33] predicted the experimental data with the mean deviation of around 30% for both macro- and mini-channel.

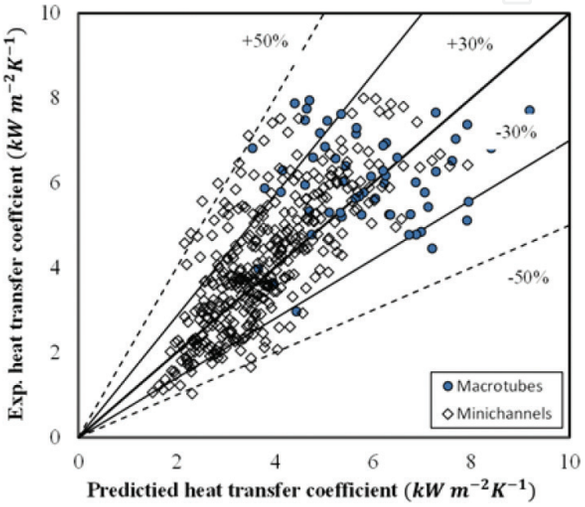

Figure 12. Comparison between experimental and predicted heat transfer coefficient.

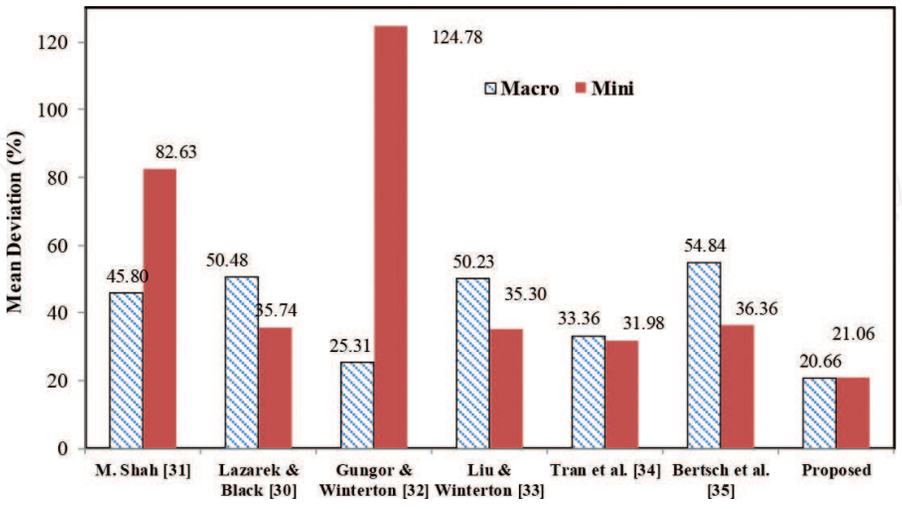

Figure 13. Summary of mean deviation.

http://dx.doi.org/10.5772/65966

4. Conclusions

The boiling heat transfer coefficient and pressure drop characteristics of R410A in horizontal tube with the inner diameter of 1.5, 3.0, 6.61 and 7.49 mm were demonstrated in this chapter. The data of heat fluxes ranging from 10 to 40 kW/m^2, mass fluxes ranging from 100 to 600 kgm^2/s, the vapour quality up to 1.0 and the saturation temperatures of 5–15°C. The results can be summarised as follows:

- The pressure drop of R410A is strongly affected by the mass flux, vapour quality and the inner tube diameter but the heat flux.
- The boiling heat transfer coefficient of R410A increased with the increase in mass flux, heat flux and the decreasing of inner tube diameter. However, in mini-channel, the effect of mass flux is only observed at the moderate quality regime, which indicates the predominance of nucleate boiling mechanism in mini-channel.
- The experimental pressure drop data were validated with some well-known correlations. Among them, the one developed by Gronnerud [20] showed the best prediction. A modified frictional pressure drop was proposed with the mean deviation of 9.29% versus the present data.
- The two-phase boiling heat transfer coefficient data were also compared with various general correlations. A new heat transfer coefficient correlation was also proposed that archived the good deviation versus the experimental data.

Nomenclature

A: Area (m^2)

AD: Average deviation, $\mathrm{AD} = \left(\frac{1}{n}\right)\sum_{1}^{n}\left(\left(\mathrm{d}p_{\mathrm{pred}} - \mathrm{d}p_{\mathrm{exp}}\right) \times 100 / \mathrm{d}p_{\mathrm{exp}}\right)$

Bo: Boiling number, $\mathrm{Bo} = \frac{q}{Gi_{\mathrm{fg}}}$

C: Chisholm parameter

c_{p}: Specific heat (kJ kg^{-1} K^{-1})

D: Diameter (m)

f: Friction factor

G: Mass flux (kg m^{-2} s^{-1})

g: Acceleration due to gravity (m s^{-2})

h: Heat transfer coefficient (kW m^{-2} K^{-1})

i: Enthalpy (kJ kg^{-1})

L: Tube Length (m)

MD: Mean deviation, $\mathrm{MD} = \left(\frac{1}{n}\right)\sum_{1}^{n}\left|\left(\left(\mathrm{d}p_{\mathrm{pred}} - \mathrm{d}p_{\mathrm{exp}}\right)\times 100 / \mathrm{d}p_{\mathrm{exp}}\right)\right|$

M: Molecular weight (kg kmol^{-1})

n: Number of data

p: Pressure (kPa)

Q: Electric power (kW)

q: Heat flux (kW m^{-2})

Re: Reynolds number, $\mathrm{Re} = \frac{GD}{\mu}$

RMS: Root mean square

T: Temperature (K)

$\dot{m}$: Mass flow rate (kg s^{-1})

X: Lockhart-Martinelli parameter

x: Vapour quality

z: Length (m)

Greek letters

α: Void fraction

Δi: The enthalpy rise across the tube (kJ kg^{-1})

μ: Dynamic viscosity (N s m^{-2})

ρ: Density (kg m^{-3})

σ: Surface tension (N m^{-1})

ϕ^2: Two-phase frictional multiplier

Gradients and differences

(dp/dz): Pressure gradient (N m^{-2} m^{-1})

(dp/dz F): Pressure gradient due to friction (N m^{-2}m^{-1})

http://dx.doi.org/10.5772/65966

Subscripts

crit: Critical point

exp: Experimental value

f: Saturated liquid

fi: Inlet liquid

g: Saturated vapour

i: Inner tube

lo: Liquid only

o: Outlet tube

pb: Pool boiling

pred: Prediction value

r: Reduced

sat: Saturation

sc: Subcooled

t: Turbulent

tp: Two-phase

v: Laminar

w: Wall

wi: Inside tube wall

Acknowledgement

This research was supported by Basic Science Research Program through the National Research Foundation of Korea (NRF) funded by Ministry of Education, Science and Technology (NRF-2016R1D1A1A09919697).

Author details

Jong-Taek Oh*[1], Nguyen Ba Chien[2], Kwang-Il Choi[1] and Pham Quang Vu[2]

*Address all correspondence to: ohjt@chonnam.ac.kr

1 Department of Refrigeration and Air-Conditioning, Chonnam National University, Yeosu, Chonnam, South Korea

2 Graduate School, Chonnam National University, Yeosu, Chonnam, South Korea

References

[1] Yongchan, K., Kookjeong, S., Jin, T. C. (2002). Evaporation heat transfer characteristics of R-410A in 7 and 9.52 mm smooth/micro-fine tubes. Int. J. Refrigeration, 25, 716–730.

[2] Man-Hoe, K., Joeng-Seob, S. (2005). Evaporating heat transfer of R22 and R410A in horizontal smooth and micro tubes. Int. J. Refrigeration, 28, 940–948.

[3] Wellsandt, S., Vamling, L. (2005). Evaporation of R407C and R410A in a horizontal herringbone microfin tube: heat transfer and pressure drop. Int. J. Refrigeration, 28, 901–911.

[4] Park, C. Y., Hrnjak, P. S. (2007). CO2 and R410A flow boiling heat transfer, pressure drop, and flow pattern at low temperatures in a horizontal smooth tube. Int. J. Refrigeration, 30(1), 166–178.

[5] Padovan, A., Del Col, D., Rossetto, L. (2011). Experimental study on flow boiling of R134a and R410A in a horizontal microfin tube at high saturation temperatures. Appl. Therm. Eng., 31(17–18), 3814–3826.

[6] Cavallini, A., Del Col, D., Doretti, L., Matkovic, M., Rossetto, L., Zilio, C. (2005). Two-phase frictional pressure gradient of R236ea, R134a and R410A inside multi-port mini-channels. Exp. Therm. Fluid Sci., 29(7), 861–870.

[7] Kaew-On, J., Wongwises, S. (2009). Experimental investigation of evaporation heat transfer coefficient and pressure drop of R-410A in a multiport mini-channel. Int. J. Refrigeration, 32(1), 124–137.

[8] C. Nguyen, V. Pham, Choi, K-I, OH, J-T, Heat Transfer Coefficient and Pressure Drop of R410A During Evaporation Inside Aluminum Multiport Minichannels, in: Vol. 2 Photovoltaics; Renewable-Non-Renewable Hybrid Power Syst. Smart Grid, Micro-Grid Concepts; Energy Storage; Sol. Chem. Sol. Heat. Cool. Sustain. Cities Communities, Transp. Symp. Integr. Buil, ASME, 2015: p. V002T18A004

[9] Choi, K.-I., Pamitran, A. S., Oh, C.-Y., Oh, J.-T. (2008). Two-phase pressure drop of R-410A in horizontal smooth minichannels. Int. J. Refrigeration, 31(1), 119–129.

[10] Oh, J. T., Pamitran, A. S., Choi, K. I., Hrnjak, P. (2011). Experimental investigation on two-phase flow boiling heat transfer of five refrigerants in horizontal small tubes of 0.5, 1.5 and 3.0 mm inner diameters. Int. J. Heat Mass Transf., 54(9–10), 2080–2088.

[11] Chien, N. B., Vu, P. Q., Choi, K.-I., Oh, J.-T. (2015). A general correlation to predict the flow boiling heat transfer of R410A in macro-/mini-channels. Sci. Technol. Built Environ., 21(5), 526–534.

[12] Lemmon, E. W., Huber, M. L., McLinden, M. O. (2007). NIST standard reference database 23: reference fluid thermodynamic and transport properties-REFPROP, Version 8.0. National Institute of Standards and Technology, USA.

[13] Steiner, D. (1993). Heat transfer to boiling saturated liquids. VDI Heat Atlas 1st edition. Society Process Engineering and Chemical Engineering. Springer-Verlag Berlin Heidelberg. (Translator: J. W. Fullarton, Dusseldorf.)

[14] Rouhani, Z., Axelsson, E. (1970). Calculation of volume void fraction in subcooled and quality region. Int. J. Heat Mass Transf., 13, 383–393.

[15] Choi, K.-I., Pamitran, A. S., Oh, J.-T., Saito, K. (2009). Pressure drop and heat transfer during two-phase flow vaporization of propane in horizontal smooth minichannels. Int. J. Refrigeration, 32(5), 837–845.

[16] Zhao, Y., Molki, M., Ohadi, M. M., Dessiatoun, S. V. (2000). Flow boiling of CO2 in microchannels. ASHRAE Trans. 106(Part 1), 437–445.

[17] Yoon, S. H., Cho, E. S., Hwang, Y. W., Kim, M. S., Min, K., Kim, Y. (2004). Characteristics of evaporative heat transfer and pressure drop of carbon dioxide and correlation development. Int. J. Refrigeration, 27, 111–119.

[18] Oh, H. K., Ku, H. G., Roh, G. S., Son, C. H., Park, S. J. (2008). Flow boiling heat transfer characteristics of carbon dioxide in a horizontal tube. Appl. Therm. Eng., 28, 1022–1030.

[19] Cho, J. M., Kim, M. S. (2007). Experimental studies on the evaporative heat transfer and pressure drop of CO2 in smooth and micro-fin tubes of the diameters of 5 and 9.52 mm. Int. J. Refrigeration, 30, 986–994.

[20] Gronnerud, R. (1972). Investigation in liquid holdup, flow resistance and heat transfer in circular type evaporator, part IV: two-phase resistance in boiling refrigerant. Bulletin de l'Inst du Froid, Annexe, 1972.

[21] Chisholm, D. (1973). Pressure gradient due to the friction during the flow of evaporating two-phase mixture in smooth tubes and channel. Int. J. Heat Mass Transf., 16, 347–358.

[22] Friedel, L. (1979). Improve friction pressure drop correlation for horizontal and vertical two-phase pipe flow. European Two-Phase Flow Group Meeting, Ispra, Italia, June, Paper E2.

[23] Muller-Steinhagen, H., Heck, K. (1986). A simple friction pressure drop correlation for two phase flow in pipe. Chem. End. Process., 20, 297–308.

[24] Lockhart, R. W., Martinelli, R. C. (1949). Proposed correlation of data for isothermal two-phase, two-component flow in pipes. Chem. Eng. Prog., 45, 39–48.

[25] Kew, P. A., Cornwell, K. (1997). Correlations for the prediction of boiling heat transfer in small-diameter channels. Appl. Therm. Eng., 17(8–10), 705–715.

[26] Lazarek, G. M., Black, S. H. (1982). Evaporative heat transfer, pressure drop and critical heat flux in a small diameter vertical tube with R-113. Int. J. Heat Mass Transf., 25, 945–960.

[27] Wambsganss, M. W., France, D. M., Jendrzejczyk, J. A., Tran, T. N. (1993). Boiling heat transfer in a horizontal small-diameter tube. J. Heat Transf., 115, 963–975.

[28] Tran, T. N., Wambsganss, M. W., France, D. M. (1996). Small circular-and rectangular-channel boiling with two refrigerants. Int. J. Multiphase Flow, 22(3), 485–498.

[29] Mastrullo, R., Mauro, A. W., Thome, J. R., Toto, D., Vanoli, G. P. (2012). Flow pattern maps for convective boiling of CO2 and R410A in a horizontal smooth tube: experiments and new correlations analyzing the effect of the reduced pressure. Int. J. Heat Mass Transf., 55(5–6), 1519–1528.

[30] Shah, M. M. (1982). Chart correlation for saturated boiling heat transfer: equations and further study. ASHRAE Trans. (United States), 88(1), 185–196.

[31] Gungor, K., Winterton, R. (1986). A general correlation for flow boiling in tubes and annuli. Int. J. Heat Mass Transf., 29(3), 351–358.

[32] Liu, Z., Winterton, R. (1991). A general correlation for saturated and subcooled flow boiling in tubes and annuli, based on a nucleate pool boiling equation. Int. J. Heat Mass Transf., 34(11), 2759–2766.

[33] Tran, T., Wambsganss, M., France, D. (1996). Small circular-and rectangular-channel boiling with two refrigerants. Int. J. Multiphase Flow, 3(4), 485–498.

[34] Bertsch, S. S., Groll, E. A., Garimella, S. V. (2009). A composite heat transfer correlation for saturated flow boiling in small channels. Int. J Heat Mass Transf., 52(7–8), 2110–2118.

[35] Kandlikar, S. (1990). A general correlation for saturated two-phase flow boiling heat transfer inside horizontal and vertical tubes. J. Heat Transf., 112(1), pp. 219–228.

[36] Kandlikar, S., Steinke, M. (2003). Predicting heat transfer during flow boiling in minichannels and microchannels, ASHRAE Trans., 109, 667–676.

[37] Chen, J. C. (1966). A correlation for boiling heat transfer to saturated fluids in convective flow. Ind. Eng. Chem. Process Des. Dev., 5, 322–329.

[38] Dittus, F. W., Boelter, L. M. K. (1930). Heat transfer in automobile radiators of the turbulent type. Univ. Calif. Publ. Eng., 2, 443–461.

[39] Cooper, M. G. (1984). Heat flow rates in saturated nucleate pool boiling e a wide-ranging examination using reduced properties. Adv. Heat Transf., 16, 157–239.